Spinal voltage-gated potassium channel Kv1.3 contributes to neuropathic pain via promotion of microglial M1 polarization and activation of the NLRP3 inflammasome

Spinal voltage-gated potassium channel Kv1.3 contributes to neuropathic pain via promotion of microglial M1 polarization and activation of the NLRP3 inflammasome

Xiaoman Yuan[1], Siyi Han[1], Anne Manyande[2], Feng Gao[1], Jie Wang[3], Wen Zhang[1*a], Xuebi Tian[1*a]

1.Department of Anesthesiology, Tongji Hospital, Tongji Medical College, Huazhong University of Science and Technology;

2. School of Human and Social Sciences, University of West London, London, UK

3. State Key Laboratory of Magnetic Resonance and Atomic and Molecular Physics, Key Laboratory of Magnetic Resonance in Biological Systems, Wuhan Center for Magnetic Resonance, Wuhan Institute of Physics and Mathematics, Chinese Academy of Sciences, Wuhan, China

*** Corresponding author**

Xuebi Tian : Address: Jiefang Avnue 1095#, Wuhan, Hubei, China 430030; Tel.:1011862783663423; fax: 1011862783662853. E-mail address:tianxb@hust.edu.cn

Keywords: microglial activition$_1$, M1 polarization$_2$, neuropathic pain$_3$, Kv1.3$_4$, the NLRP3 inflammasome$_5$, neuroinflammation$_6$.

[a] Wen Zhang and Xuebi Tian contributed equally to this work

15 **Abstract**

16 Studies have shown that activation of microglia is the main mechanism of neuropathic pain. Kv1.3
17 channel is a novel therapeutic target for treating neuroinflammatory disorders due to its crucial role in
18 subsets of microglial cells. As such, it may be involved in the processes of neuropathic pain, however,
19 whether Kv1.3 plays a role in neuroinflammation following peripheral nerve injury is unclear. The
20 spared nerve injury model (SNI) was used to establish neuropathic pain. Western blot and
21 immunofluorescence were used to examine the effect of Kv1.3 in the SNI rats. PAP-1, a Kv1.3 specific
22 blocker was administered to alleviate neuropathic pain in the SNI rats. Neuropathic pain and allodynia
23 occurred after SNI, the levels of M1 (CD68, iNos) and M2 (CD206, Arg-1) phenotypes were up-
24 regulated in the spinal cord, and the protein levels of NLRP3, caspase-1 and IL-1β were also increased.
25 Pharmacological blocking of Kv1.3 with PAP-1 alleviated hyperpathia induced by SNI. Meanwhile,
26 intrathecal injection of PAP-1 reduced M1 polarization and decreased NLRP3, caspase-1, and IL-1β
27 expressions of protein levels. Our research indicates that the Kv1.3 channel in the spinal cord
28 contributes to neuropathic pain by promoting microglial M1 polarization and activating the NLRP3
29 inflammasome.

30

31 **1 Introduction**

32 Neuropathic pain is a primary subgroup of pathological pain that results from a lesion or disease of
33 somatosensory system(Baron R et al., 2010).Hyperpathia, allodynia, and spontaneous pain are the main
34 clinical symptoms of neuropathic pain(Jensen TS and Finnerup NB, 2014) .Studies have shown many
35 adverse effects of chronic pain on prognosis and mental health(Geneen LJ et al., 2017;Treede RD et
36 al., 2019) .Unfortunately, the mechanisms of nerve injury that induce neuropathic pain are extremely
37 complicated, and there is a lack of preventive and therapeutic measures(Cohen S and Mao J,

2014;Gilron I et al., 2006) .Therefore, it is necessary to further explore the mechanisms and find a novel treatment that can target neuropathic pain.

Kv1.3 channel is a classic voltage-gated potassium channel highly expressed in microglia. It also plays a crucial role in inflammatory responses(Sarkar S et al., 2020)via promoting release of inflammatory cytokines and oxidative stress(Varga Z et al., 2021),which eventually induces loss of neurons(Fordyce CB et al., 2005).A recent study showed that Kv1.3 was upregulated in activated microglia(Rangaraju S et al., 2015).In addition, Kv1.3 channel is considered a novel therapeutic target for treating neuroinflammatory disorders due to its crucial role in subsets of T lymphocytes as well as microglial cells(Tubert C et al., 2016).However, it is not clear whether Kv1.3 is involved in neuropathic pain via shifting microglial phenotype and inducing inflammation.

Rodent models suggest that neuroinflammation contributes to neuropathic pain(Ellis A and Bennett DLH, 2013) .Initial work focused on the idea that microglia can drive neuroinflammation(Muzio L et al., 2021).Many research reports have demonstrated that microglia is involved in regulating various types of chronic pain(Chen G et al., 2018;Tan Y-H et al., 2012),such as neuropathic pain(Pike AF et al., 2022) and inflammatory pain(Decosterd I and Woolf CJ, 2000).Microglia appear to be heterogeneous with two functional phenotypes:M1 phenotype and M2 phenotype, which produce cytotoxic or neuroprotective effects, respectively(Song Z et al., 2017;Xiong B et al., 2020).Blocking Kv1.3 channel with PAP-1 increased levels of anti-inflammatory M2 phenotype microglia and inhibited M1 phenotypes in MCAO(middle cerebral artery occlusion), POCD (Postoperative cognitive dysfunction), and DIO(diet-induced obsisity) models(Rangaraju et al. 2015).However, the roles of M1 and M2 microglia in neuropathic pain are unclear.

The NLRP3 inflammasome was found to process damaged signals to trigger the inflammatory response(Doyle TM et al., 2019).A plethora of studies have shown that the NLRP3 inflammasome

plays a central role in neuroinflammation induced by injury(Hu X et al., 2021;Kelley N et al., 2019;Liu X et al., 2021). Mechanistic connections between the NLRP3 inflammasome and Kv1.3 are becoming increasingly clear(Pike AF et al., 2022).Here, we hypothesized that Kv1.3 channel in the spinal cord can promote M1 microglial polarization and activate the NLRP3 inflammasome which results in neuropathic pain in rats. Using the SNI model and treatment with PAP-1, We first examined changes in M1 and M2 microglia in the spinal cord after SNI. Then, we investigated the role of Kv1.3 in regulating M1/M2 transformation, using PAP-1. Lastly, we examined whether Kv1.3 channel blockade exerts a neuroprotective effect through suppressing the NLRP3 inflammasome activation during SNI.These findings may provide laboratory support for translational studies in neuropathic pain of Kv1.3 inhibitors.

2 Materials and methods

2.1 Animals

A total of 142 Male SD (6–8 weeks, 200-250 g) rats were supplied from Tongji Hospital, Tongji Medical College, Huazhong University of Science and Technology, Wuhan, Hubei, China. All animals were raised under controlled conditions (22–25 °C, 12-hour alternate circadian rhythm, free access to food and water, 3-4 rats per cage). All animal studies followed the protocol approved by the Animal Care and Use Committee of Tongji Hospital.

2.2 Induction of neuropathic pain

SNI models were established according to the procedures previously described(Decosterd I and Woolf CJ, 2000). The left sciatic nerve (containing the three branches: common peroneal, tibial, and sural nerve) was exposed after rat was anesthetized with pentobarbital sodium (50 mg/kg, intraperitoneally). The two branches of the sciatic nerve (the common peroneal nerve and the tibial nerve) were tightly ligated with a 5.0 silk thread (or suture) and sectioned distal to the ligation, removing 2±4 mm of the

84 distal nerve stump. The intact sural nerve was carefully avoided by preventing any contact or straining.
85 Then the skin was closed. In the SHAM group, the sciatic nerve was just exposed without being ligated
86 or sectioned.

87 **2.3 Pain behavioral test**

88 The mechanical paw withdrawal threshold (MPWT) of the ipsilateral hind paw was determined using
89 Von Frey filament, which simulated mechanical allodynia as previously described. All behavioral tests
90 took place between 8:30 a.m. and 4:30 p.m. Briefly, mice were placed in individual plastic enclosures
91 on a metal mesh floor and given 30 minutes to acclimate. Positive responses included abrupt paw
92 withdrawal, licking, and shaking. The MPWT was measured as previously describe(Song Z et al.,
93 2016) and was defined as the least amount of force required to elicit a positive response (in grams).
94 All behavioral tests were carried out by a researcher who was unaware of the study's design.

95 **2.4 Western blot analysis**

96 The procedure for collecting spinal tissue and preparing spinal protein samples had previously been
97 followed(Xiong B et al., 2020).Equal amounts of spinal protein samples were separated using 10
98 percent sodium dodecyl sulfate-polyacrylamide gel electrophoresis (SDS-PAGE) and then
99 electroblotted using Millipore polyvinylidene fluoride membranes. The membranes were blocked for
100 1 hour at room temperature (RT) with 5% skim milk or BSA in Tris-buffered saline and Tween 20
101 (TBST, 0.1%), incubated with primary antibody overnight at 4 °C and then incubated for 1 hour at RT
102 with horseradish peroxidase (HRP)-conjugated goat anti-mouse secondary antibody (1:5000 ABclonal,
103 AS003), goat anti-rabbit secondary antibody (1:5000 ABclonal, AS014), rabbit anti-goat secondary
104 antibody (1:5000 ABclonal, AS029). The specific primary antibodies used in this study including:
105 GAPDH (1:1000 ABclonal, A19056), iba-1 (1:1000 abcam, ab5076), IL-1β (1:1000 ABclonal,
106 A1112), Arg-1 (1:1000 ABclonal, A4923), caspase-1 (1:1000 protentech, 22915-1-AP), Kv1.3 (1:400

santa, sc-398855), CD68 (1;1000 abcam, ab125212), CD206 (1:1000 abcam, ab203490), iNos (abcam, ab283655), NLRP3 (1:1000 HUABIO, ET1610-93). Chemiluminescence (Pierce ECL Western Blotting Substrate; Thermo Scientific) was used to evaluate the protein bands, and a computerized image analysis system (ChemiDoc XRS+; BIO-RAD) was used to measure them.

2.5 Immunofluorescence staining

The rats were severely sedated with an overdose of isoflurane and transcardially perfused with phosphate-buffered saline (PBS), followed by 4% paraformaldehyde. The spinal cord was removed and preserved at 4 °C with 4% paraformaldehyde. Using a cryostat microtome, the fixed spinal cord was sectioned into 20 μm thick coronal slices (Thermo Fisher, NX50, Waltham, MA). PBS was used to wash free-floating slices at first (3 times, 8 min each). The slices were washed and incubated for 1 hour at 37 °C in blocking buffer (10% normal goat serum, 0.3% Triton X-100 in PBS). After blocking, the slices were treated with primary antibodies for 72 hours at 4 °C, including: iba-1 (1:400 abcam ab5076), CD68 (1:100 abcam, ab125212), Arg-1 (1:50 CST, 93668), iNos (1:100 abcam, ab283655), CD206 (1:200 abcam, ab203490), or NLRP3 (1:500 HUABIO, ET1610-93). And then, the sections were incubated with a Cy3-conjugated (1:200 Jackson, 711-165-152), or 488-conjugated secondary antibody (1:200 Jackson, 155707) for 2 hours at 37 °C, stained with DAPI for 10 min at RT, washed with PBS (3 times, 10 min each). Finally, a virtual microscopy slide scanning system was used to view the immunostained brain slice (Olympus, VS 120, Tokyo, Japan). Using ImageJ, images of slices containing the region of interest (ROI) were cropped and counted (National Institutes of Health, Bethesda, MD). Image J was used to quantify the cells. The average number of double-labeled cells per square millimeter in each group was used to calculate the density of double-labeled cells.

2.6 Experimental designs and drugs treatment

This study was designed as demonstrated in Figure 1A and Figure 2A. First, we examined the protein levels of Kv1.3 in the spinal cord. Next, we further tested the activation of microglia and the NLPR3 inflammasomes in the spinal cord. Then, PAP-1 (5 μg, sigma) or Vehicle was intrathecally(i.t.) administered from day 7 to day 12 after surgery to explore whether it alleviated hyperpathia in the SNI rats. we designed three drug administration methods to explore the therapeutic effect of PAP-1 in neuropathic pain, which include a single dose (2.5 μg/100g), multiple doses (2.5 μg/100g,5 days), and a prophylactic dose (2.5 μg/100g, 5 days). A pre-experiment was used to determine the PAP-1 dosage, such as (5 μg/kg, 25 μg/kg, 50 μg/kg, i.t.)(which is showed as supporting information in the supplemental material, Figure1).

2.7 Statistical analysis

All results are shown as mean ±SEM. For analyses, when comparing two groups, an unpaired Student's *t*-test was used, for multiple groups, one-way ANOVA followed by the Bonferroni post hoc test was utilized. Two-way ANOVA followed by Bonferroni post hoc test was used to analyze the MPWT. Pearson coefficients were applied to statistically express pertinence. GraphPad Prism 7.0 was used for statistical analysis, and $P < 0.05$ was considered statistically significant in this study.

3 Results

3.1 SNI caused mechanical allodynia and increase of Kv1.3 in the spinal cord

To evaluate the development of mechanical allodynia after SNI, the MPWT was tested on day 0, day 1, day 3, day 7, and day 14 (fig1A). The results obtained are consistent with our previous results of similar studies that the MPWT was distinctly decreased in the SNI rats compared to the SHAM group (fig1B). Next, we examined the protein levels of Kv1.3 channel in the spinal cord by western blot. The results showed that the expression of Kv1.3 was increased on day 1 and continued up until day 14 after

151 SNI (fig1C). Then, immunofluorescence was used to detect the co-localization of Kv1.3 and microglia
152 (iba-1). Kv1.3 was extensively co-localized with iba-1 in the spinal cord, and the immunoreactivity
153 was increased after SNI (fig1D). These results indicate that the protein expression of Kv1.3 was
154 increased and co-localized with microglia in the spinal cord of the SNI rats.

155 **3.2 PAP-1 reversed mechanical allodynia caused by neuropathic pain**

156 PAP-1 is the selective inhibitor of Kv1.3. We then used PAP-1 to further study the role of Kv1.3 in
157 neuropathic pain. At the same time, the MPWT was performed after using PAP-1(fig2A). Drug dose
158 and Tmax (peak time of drug) were obtained by pre-experiment (which is showed as supporting
159 information in the supplemental material). The results suggest that a single administration of PAP-1
160 after SNI could effectively increase the MPWT and continued for 6 hours (fig2B). In addition,
161 continuous use of PAP-1 7 days after establishing the model can also improve mechanical allodynia of
162 the SNI rats (fig2C). However, prophylactic use of PAP-1 had no effect on the MPWT of the SNI rats
163 (fig2D). Next, the expression of Kv1.3 was examined by western blot. The result showed that
164 administration of PAP-1 clearly decreased the level of PAP-1 in the spinal cord of the SNI rats. As a
165 result, we concluded that PAP-1 can decrease the level of Kv1.3 protein and increase the MPWT in the
166 SNI rats.

167 **3.3 Microglia were activated in the spinal cord of the SNI rats**

168 Kv1.3 channel is highly expressed in microglia and is a key therapeutic target for inflammatory
169 diseases. Next, microglia expression in the spinal cord was examined by western blot and
170 immunofluorescence. The results showed that the expression of iba-1 protein was remarkably increased
171 and continued up to day 14 in the SNI rats (fig3A). Besides, compared to the SHAM group,
172 immunostaining of iba1 was enhanced and microglial bodies were enlarged with retraction of the
173 protuberances on day 3 and continued until day 14 in the spinal cord of the SNI rats (Fig3B). Then, we

174 quantitatively analyzed the mean fluorescent intensity of iba-1(fig3C) and the number of iba-1$^+$ cells
175 (fig3D) in the spinal cord. The results demonstrated that the mean fluorescent intensity and the number
176 of iba-1$^+$ cells were significantly increased after SNI, compared with the SHAM group. These results
177 indicate that microglia are activated in the spinal cord after SNI.

178 **3.4 Microglia were activated and mainly expressed as the M1 phenotype in the spinal cord**
179 **after SNI.**

180 The changes in microglia, M1 versus M2, after SNI were examined by western blot with CD68 and
181 iNos identified as markers of the M1 phenotype, and CD206, and Arg-1 as markers of the M2
182 phenotype. The results showed that compared with the SHAM group, the level of CD68 increased in a
183 time-dependent manner on days 1, 3, 7, and 14 (fig4A), while the expression of iNos significantly
184 increased in the SNI rats (fig4B). In contrast, both Arg-1 and CD206 increased early after SNI and then
185 gradually decreased to baseline by day 14 (fig4C). At the same time, we examined the colocalization
186 of iba-1 with CD68, iNos, CD206 and Arg-1(fig4E). The results revealed that the ratios of CD68$^+$ and
187 iNos$^+$ cells in microglia clearly increased in a time-dependent manner in the spinal cord of the SNI rats
188 which are consistent with western blot results (fig4F,4G). The ratio of CD206$^+$ cells in the microglia
189 increased on days 1, 3, and 7, but decreased on day 14 (fig 4H). Although, the ratio of Arg-1$^+$ cells
190 increased on day 1 and day 3, it reduced to baseline at day 7 and day 14 (fig4I). These findings indicate
191 that microglia are activated and mainly expressed as the M1 phenotype in the spinal cord after SNI.

192 **3.5 Neuroinflammation activated the NLRP3 inflammasome in the spinal cord after SNI**

193 Many researchers suggest that the NLRP3 inflammasome is activated by neuroinflammation. We next
194 examined the protein levels of NLRP3, caspase-1(p20), and IL-1β(p17) in the spinal cord. The results
195 showed that the expressions of NLRP3, caspase-1, and IL-1β increased in the spinal cord in a time-
196 dependent manner after SNI (fig5A,5B,5C). Then, we analyzed the co-location of NLRP3 and iba-1 in

197 the spinal cord. Double immunofluorescence staining of iba-1 and NLRP3 was markedly increased
198 after SNI (fig5D), and the mean fluorescent intensity was upregulated (fig5E). These results imply that
199 neuroinflammation activates the NLRP3 inflammasome after SNI which is associated with neuropathic
200 pain.

201 **3.6 PAP-1 reversed the polarization of microglia in the spinal cord of the SNI rats**

202 Next, PAP-1 was used to further investigate the role of Kv1.3 in neuroinflammation after SNI. The
203 results showed that the expression of iba-1 decreased in the spinal cord of the SNI rats after
204 administration of PAP-1(fig6A). Meanwhile, the levels of CD68 and iNos (markers of the M1
205 phenotype) were significantly downregulated after using PAP-1, but the levels of CD206 and Arg-1
206 (markers of the M2 phenotype) were upregulated (fig6B,6C,6D,6E). Similarly, the results of
207 immunofluorescence were consistent with those of western blot (fig6F). The level of iba-1+ cells
208 decreased particularly those of CD68+/iba-1+ and iNos+/iba-1+ cells, while the levels of CD206+/iba-
209 1+ and Arg-1+/iba-1+ cells increased in the spinal cord of the SNI rats after using PAP-
210 1(fig6G,6H,6I,6J,6K). These results suggest that PAP-1 reverses the polarization of microglia induced
211 by upregulation of Kv1.3 channel in the spinal cord of the SNI rats.

212 **3.7 PAP-1 reversed activation of the NLRP3 inflammasome in the spinal cord of the SNI rats**

213 Blockade of Kv1.3 with PAP-1 reversed the polarization of M1 microglia in the SNI rats. Subsequently,
214 we examined the expression of the NLRP3 inflammasome by western blot and immunofluorescence.
215 The results showed that the expressions of NLRP3, caspase-1, and IL-1β decreased remarkably after
216 administration of PAP-1 in the SNI rats (fig7A,7B,7C). The mean fluorescent intensity of NLRP3/iba-
217 1 was also reduced in the SNI rats after using PAP-1 (fig7D, 7E). These results denote that PAP-1
218 effectively reverses activation of the NLRP3 inflammasome in the SNI rats.

219 **4 Discussion**

Neuropathic pain is a clinically intractable disease that seriously affects patients' quality of life. In the present study, we used PAP-1 as a tool to examine the role of Kv1.3 in microglia in neuropathic pain. Our results showed that PAP-1 attenuated SNI-induced microglial polarization, neuroinflammation, and allodynia. We found that PAP-1 reduced SNI-induced Kv1.3 upregulation and NLRP3 production, reverted the ratio of M1/M2 reactive microglia in the spinal cord, and relieved mechanical allodynia after peripheral injury. These results demonstrate that Kv1.3 contributes to neuropathic pain via promotion of microglial M1 polarization and activation of the NLRP3 inflammasome.

Kv1.3 was first described in human T-cells, where it regulates T-cell activation(Panyi G, 2005). Other immune cells include macrophages and B cells, which can express Kv1.3 under specific conditions(Beeton C et al., 2006) . It is notable that a systems pharmacology-based study identified functional roles for Kv1.3 in pro-inflammatory microglial activation(Di Lucente J et al., 2018). Increase of microglial Kv1.3 expression has been observed in both human and rodent models of Alzheimer's disease (AD)(Rangaraju S et al., 2015) and Parkinson's disease (PD)(Tubert C et al., 2016) , suggesting that Kv1.3 may be an effective strategy for reducing neuroinflammation in the context of a variety of central nervous system diseases. Kv1.3 inhibitors have also been shown to ameliorate disease severity and neurologic deficit in rodent models of ischemic stroke(Ma D-C et al., 2020). Similarly, PAP-1 treatment reduced neuroinflammation, decreased cerebral amyloid load, enhanced hippocampal neuronal plasticity, and improved behavioral deficits in mouse models of AD(Du Y et al., 2021). Peimine, one of the main components in Fritillaria which has a long history of use as an anti-inflammatory and pain-relieving herb in ancient Chinese medical practice, was found to be able to inhibit Kv1.3 channels(Xu J et al., 2016). Similar to non-steroidal anti-inflammatory drugs (NSAIDs) it could effectively suppress the Kv1.3 currents in T-lymphocytes and thus exerted immunosuppressive effects to more rapidly reduce headache after vaccination(Kazama I and Senzaki M, 2021). But it is not clear whether the neuropathic pain and allodynia induced by SNI are attributable

244 to the effects of Kv1.3 of microglia. In our study, SNI induced an on-going upregulation of Kv1.3 in
245 the spinal cord and PAP-1 effectively increased the MPWT of the SNI rats. An interesting finding is
246 that preventive treatment with PAP-1 before establishing SNI model could not prevent the development
247 of SNI. Possibly, since the small molecule Kv1.3 blocker PAP-1 is lipophilic(Lam J and Wulff H,
248 2011) and the t1/2 of PAP-1 in rodents is short (3.8 hours) (Beeton C et al., 2006). The pharmaceutical
249 concentration of preventive treatment is unamenable to play an instant immunosuppressive role in
250 alleviating mechanical allodynia after surgery. The decrease of the MPWT at 6 hours after a single
251 dose seems also to confirm this. However, continuous administration of PAP-1 for 5 days after surgery
252 remarkably reversed the mechanical allodynia and maintained this effect in the SNI rats, indicating that
253 blocking Kv1.3 could prevent neuropathic pain through a blocking process such as neuroinflammation.
254 As alluded to earlier, Kv1.3 plays an important role in immune cell activation in nervous system
255 diseases through the high expression of pro-inflammatory microglia(Felipe A, 2018). In the present
256 study, we observed an imbalanced microglial polarization of M1 and M2 in the spinal cord of the SNI
257 model. Alterations in M1/M2 polarization are associated with excessive inflammatory
258 activation(Orihuela R et al., 2016) and may play an important role in the development and progression
259 of SNI. Indeed, we found that during the development of SNI, reactive microglia were mainly
260 expressed as M1 microglia, with very few M2 microglia. It is pertinent that lipopolysaccharide(LPS)-
261 induced microglial activation, which transforms into classical ("M1") phenotype, has been shown to
262 require the participation of microglial Kv1.3(Di Lucente J et al., 2018).In mice genetically devoid of
263 Kv1.3, LPS failed to activate microglia, or produce neuroinflammation(Nicolazzo JA et al., 2022).
264 Progranulin could inhibit LPS-induced macrophage M1 polarization via NF-κB and MAPK signaling
265 pathways(Liu L et al., 2020). But whether Kv1.3 channel is associated with the reshaping of microglial
266 phenotype in neuropathic pain is still unclear. Our findings showed that the expression of M1 microglia
267 was reduced, and the expression of M2 was increased when mechanical allodynia was relieved in the
268 SNI rats after intrathecal injection of PAP-1. These results suggest that Kv1.3 contributes to

neuropathic pain via the promotion of microglial M1 polarization. Activation of Kv1.3 channel in cytomembrane induces K^+ efflux, while the low intracellular potassium concentration has a fundamental role in activating the NLRP3 inflammasome(He Y et al., 2016). It has been acknowledged that the NLRP3 inflammasome activation mediates inflammatory responses after nerve injury(Chen R et al., 2021). Thus, it seems plausible to infer that Kv1.3 channel may play a role in the NLRP3 inflammasome activation in microglia after nerve injury, however, there is a paucity of studies in this area. Given that the cleavage of caspase-1 and IL-1β are the hallmarks of inflammasome activation and IL-1β is a well-known pain-inducing molecule(Starobova H et al., 2020), the effect of Kv1.3 on them was investigated in the present study. Our data provides the first evidence about the association of Kv1.3 with the NLRP3 inflammasome activation in microglia after SNI. Therefore, we concluded that blockage of cellular K^+ efflux with PAP-1 may inhibit the decrease of intracellular potassium concentration, thus compromising the NLRP3 inflammasome activation after SNI in the current study. But we noticed that there was an expression peak of IL-1β on the first day after SNI. This discrepancy of IL-1β might be due to microglia and neurons responding at different times after damage(de Rivero Vaccari JP et al., 2009).

It must be admitted that there are some limitations in our study. Firstly, iba1, CD68, iNos, Arg-1, and CD206 were used to isolate microglia and identify microglial phenotypes in the present study. Although they have been used as molecular markers of activated microglia, they are not specific to microglia. These markers are also expressed by the central nervous system monocyte-derived macrophages(Crain JM et al., 2013). Thus, additional experiments such as morphology analysis are warranted to illustrate the effects of Kv1.3 blockade on microglial activation. Secondly, the initial concept of M1 or M2 phenotype is set in macrophages for experimental examination of inflammation. Although it has utility in describing microglial heterogeneity on inflammatory responses(Ransohoff RM, 2016). To translate the paradigm to microglia, efforts towards characterization would include

293 assessing the morphological phenotype, discriminating between microglia (resident macrophages) and
294 macrophages (infiltrating macrophages), metabolism, and functional features of the cells. Thirdly, it
295 has become clear that any efforts to classify microglia in distinct activation or polarized states cannot
296 rely on the standard M1/M2 polarization paradigm, but rather will require more complex phenotypes,
297 especially in vivo. Lastly, in the present study, the relationship among Kv1.3, the NLRP3
298 inflammasome activation and M1 polarization was indirectly demonstrated by the transformation of
299 biomarkers. Future studies are still warranted to examine the interrelationship of Kv1.3 effects on
300 activation of the NLRP3 inflammasome and M1 polarization, which will provide the real evidence.

301 ## 5 Conclusion

302 In conclusion, PAP-1, the Kv1.3 blocker, significantly attenuated mechanical allodynia of SNI. The
303 present study provided evidence that Kv1.3 contributes to neuropathic pain via the promotion of
304 microglial M1 polarization and activation of the NLRP3 inflammasome (fig8). Pharmacological
305 inhibition of Kv1.3 may thus, be a promising strategy in the treatment of neuropathic pain and PAP-1
306 may provide effective therapy for the management of pain in the clinic.

307 ## 6 List of abbreviations

308 MCAO :60 min of ischemia followed by reperfusion; POCD: Postoperative Cognitive Dysfunction;
309 DIO: mimicking metabolic syndrome; SNI: spared nerve injury; MPWT: The mechanical paw
310 withdrawal threshold.PAP-1: 5-(4-Phenoxybutoxy)psoralen

311 ## 7 Declarations

312 ### 7.1 Ethics approval and consent to participate

All experiments were approved by the Experimental Animal Care and Use Committee of Tongji Medical College, Huazhong University of Science and Technology, and were in agreement with the National Institutes of Health Guidelines for the Care and Use of Laboratory Animals.

7.2 Consent for publication

Not applicable.

7.3 Availability of data and materials

The data and materials supporting the conclusions of this study are available from the corresponding author on reasonable request.

7.4 Competing interests

The authors declare that they have no competing interests.

7.5 Funding

This work was supported by the National Natural Science Foundation of People's Republic of China (grant nos. 81974170) and the Natural Science Foundation of Hubei Province (grant no. 2021CFB341).

7.6 Authors' contributions

Xiaoman Yuan conceived the research, carried out the model building, performed the Western blot, coordinated the lab work and drafted the manuscript. Siyi Han and Anne Manyande performed the statistical analysis and drafted the manuscript. Feng Gao and Jie Wang took care of the MPWT and drafted the manuscript. Wen Zhang,Anne Manyande and Xue-Bi Tian participated in its design and coordination and helped to draft the manuscript. All authors read and approved the final manuscript.

7.7 Acknowledgements

The authors specially thank the Wuhan institute of physics and mathematics, the Chinese academy of sciences, the Tongji Medical College, and the Huazhong University of Science and Technology for their support and help to conduct their experiment.

8 Reference

Baron R, Binder A, Wasner G (2010), Neuropathic pain: diagnosis, pathophysiological mechanisms, and treatment. The Lancet Neurology 9:807-819.

Beeton C, Wulff H, Standifer NE, Azam P, Mullen KM, Pennington MW, Kolski-Andreaco A, Wei E, et al. (2006), Kv1.3 channels are a therapeutic target for T cell-mediated autoimmune diseases. Proc Natl Acad Sci U S A 103:17414-17419.

Beeton C, Wulff H, Standifer NE, Azam P, Mullen KM, Pennington MW, Kolski-Andreaco A, Wei E, et al. (2006), Kv1.3 channels are a therapeutic target for T cell-mediated autoimmune diseases. Proceedings of the National Academy of Sciences 103:17414-17419.

Chen G, Zhang Y-Q, Qadri YJ, Serhan CN, Ji R-R (2018), Microglia in Pain: Detrimental and Protective Roles in Pathogenesis and Resolution of Pain. Neuron 100:1292-1311.

Chen R, Yin C, Fang J, Liu B (2021), The NLRP3 inflammasome: an emerging therapeutic target for chronic pain. Journal of Neuroinflammation 18:84.

Cohen S, Mao J (2014), Neuropathic pain: Mechanisms and their clinical implications. BMJ (Clinical research ed) 348:f7656.

Crain JM, Nikodemova M, Watters JJ (2013), Microglia express distinct M1 and M2 phenotypic markers in the postnatal and adult central nervous system in male and female mice. J Neurosci Res 91:1143-1151.

de Rivero Vaccari JP, Lotocki G, Alonso OF, Bramlett HM, Dietrich WD, Keane RW (2009), Therapeutic neutralization of the NLRP1 inflammasome reduces the innate immune response and improves histopathology after traumatic brain injury. J Cereb Blood Flow Metab 29:1251-1261.

Decosterd I, Woolf CJ (2000), Spared nerve injury: an animal model of persistent peripheral neuropathic pain. Pain 87:149-158.

Di Lucente J, Nguyen H, Wulff H, Jin LW, Maezawa I (2018), The voltage - gated potassium channel Kv1.3 is required for microglial pro - inflammatory activation in vivo. Glia 66.

Di Lucente J, Nguyen HM, Wulff H, Jin L-W, Maezawa I (2018), The voltage-gated potassium channel Kv1.3 is required for microglial pro-inflammatory activation in vivo. Glia 66:1881-1895.

Doyle TM, Chen Z, Durante M, Salvemini D (2019), Activation of Sphingosine-1-Phosphate Receptor 1 in the Spinal Cord Produces Mechanohypersensitivity Through the Activation of Inflammasome and IL-1β Pathway. The Journal of Pain 20:956-964.

Du Y, Luo M, Du Y, Xu M, Yao Q, Wang K, He G (2021), Liquiritigenin Decreases Aβ Levels and Ameliorates Cognitive Decline by Regulating Microglia M1/M2 Transformation in AD Mice. Neurotox Res 39:349-358.

Ellis A, Bennett DLH (2013), Neuroinflammation and the generation of neuropathic pain. British Journal of Anaesthesia 111:26-37.

Felipe A (2018), Kv1.3 In Microglia: Neuroinflammatory Determinant and Promising Pharmaceutical Target. Journal of Neurology & Neuromedicine 3:18-23.

Fordyce CB, Jagasia R, Zhu X, Schlichter LC (2005), Microglia Kv1.3 channels contribute to their ability to kill neurons. J Neurosci 25:7139-7149.

Geneen LJ, Moore RA, Clarke C, Martin D, Colvin LA, Smith BH (2017), Physical activity and exercise for chronic pain in adults: an overview of Cochrane Reviews. Cochrane Database Syst Rev 4:CD011279-CD011279.

Gilron I, Watson CPN, Cahill CM, Moulin DE (2006), Neuropathic pain: a practical guide for the clinician. CMAJ 175:265-275.

He Y, Hara H, Núñez G (2016), Mechanism and Regulation of NLRP3 Inflammasome Activation. Trends in biochemical sciences 41:1012-1021.

Hu X, Yan J, Huang L, Araujo C, Peng J, Gao L, Liu S, Tang J, et al. (2021), INT-777 attenuates NLRP3-ASC inflammasome-mediated neuroinflammation via TGR5/cAMP/PKA signaling pathway after subarachnoid hemorrhage in rats. Brain Behav Immun 91:587-600.

Jensen TS, Finnerup NB (2014), Allodynia and hyperalgesia in neuropathic pain: clinical manifestations and mechanisms. The Lancet Neurology 13:924-935.

Kazama I, Senzaki M (2021), Does immunosuppressive property of non-steroidal anti-inflammatory drugs (NSAIDs) reduce COVID-19 vaccine-induced systemic side effects? Drug Discoveries & Therapeutics 15:278-280.

Kelley N, Jeltema D, Duan Y, He Y (2019), The NLRP3 Inflammasome: An Overview of Mechanisms of Activation and Regulation. Int J Mol Sci 20:3328.

Lam J, Wulff H (2011), The Lymphocyte Potassium Channels Kv1.3 and KCa3.1 as Targets for Immunosuppression. Drug Dev Res 72:573-584.

Liu L, Guo H, Song A, Huang J, Zhang Y, Jin S, Li S, Zhang L, et al. (2020), Progranulin inhibits LPS-induced macrophage M1 polarization via NF-κB and MAPK pathways. BMC Immunol 21:32-32.

Liu X, Zhang M, Liu H, Zhu R, He H, Zhou Y, Zhang Y, Li C, et al. (2021), Bone marrow mesenchymal stem cell-derived exosomes attenuate cerebral ischemia-reperfusion injury-induced neuroinflammation and pyroptosis by modulating microglia M1/M2 phenotypes. Experimental Neurology 341:113700.

Ma D-C, Zhang N-N, Zhang Y-N, Chen H-S (2020), Kv1.3 channel blockade alleviates cerebral ischemia/reperfusion injury by reshaping M1/M2 phenotypes and compromising the activation of NLRP3 inflammasome in microglia. Experimental Neurology 332:113399.

Muzio L, Viotti A, Martino G (2021), Microglia in Neuroinflammation and Neurodegeneration: From Understanding to Therapy. Front Neurosci 15:742065-742065.

Nicolazzo JA, Pan Y, Di Stefano I, Choy KHC, Reddiar SB, Low YL, Wai DCC, Norton RS, et al. (2022), Blockade of Microglial Kv1.3 Potassium Channels by the Peptide HsTX1[R14A] Attenuates Lipopolysaccharide-mediated Neuroinflammation. Journal of Pharmaceutical Sciences 111:638-647.

Orihuela R, McPherson CA, Harry GJ (2016), Microglial M1/M2 polarization and metabolic states. Br J Pharmacol 173:649-665.

411 Panyi G (2005), Biophysical and pharmacological aspects of K+ channels in T lymphocytes.
412 European biophysics journal : EBJ 34:515-529.

413 Pike AF, Szabò I, Veerhuis R, Bubacco L, The potential convergence of NLRP3 inflammasome,
414 potassium, and dopamine mechanisms in Parkinson's disease, NPJ Parkinson's disease, 2022, pp. 32.

415 Pike AF, Szabò I, Veerhuis R, Bubacco L (2022), The potential convergence of NLRP3
416 inflammasome, potassium, and dopamine mechanisms in Parkinson's disease. npj Parkinson's
417 Disease 8:32.

418 Rangaraju S, Gearing M, Jin L-W, Levey A (2015), Potassium channel Kv1.3 is highly expressed by
419 microglia in human Alzheimer's disease. J Alzheimers Dis 44:797-808.

420 Rangaraju S, Gearing M, Jin Lw, Levey AIJJoAsdJ (2015), Potassium channel Kv1.3 is highly
421 expressed by microglia in human Alzheimer's disease. 44 3:797-808.

422 Ransohoff RM (2016), A polarizing question: do M1 and M2 microglia exist? Nature Neuroscience
423 19:987-991.

424 Sarkar S, Nguyen HM, Malovic E, Luo J, Langley M, Palanisamy BN, Singh N, Manne S, et al.
425 (2020), Kv1.3 modulates neuroinflammation and neurodegeneration in Parkinson's disease. J Clin
426 Invest 130:4195-4212.

427 Song Z, Xiong B, Zheng H, Manyande A, Guan X-H, Cao F, Ren L, Zhou Y, et al. (2016), STAT1 as
428 a downstream mediator of ERK signaling contributes to bone cancer pain by regulating MHC II
429 expression in spinal microglia. Brain Behav Immun 60.

430 Song Z, Xiong B, Zheng H, Manyande A, Guan X, Cao F, Ren L, Zhou Y, et al. (2017), STAT1 as a
431 downstream mediator of ERK signaling contributes to bone cancer pain by regulating MHC II
432 expression in spinal microglia. Brain Behav Immun 60:161-173.

433 Starobova H, Nadar EI, Vetter I (2020), The NLRP3 Inflammasome: Role and Therapeutic Potential
434 in Pain Treatment. Front Physiol 11:1016-1016.

435 Tan Y-H, Li K, Chen X-Y, Cao Y, Light AR, Fu K-Y (2012), Activation of Src Family Kinases in
436 Spinal Microglia Contributes to Formalin-Induced Persistent Pain State Through p38 Pathway. The
437 Journal of Pain 13:1008-1015.

438 Treede RD, Rief W, Barke A, Aziz Q, Bennett M, Benoliel R, Cohen M, Evers S, et al. (2019),
439 Chronic pain as a symptom or a disease: the IASP Classification of Chronic Pain for the International
440 Classification of Diseases (ICD-11). PAIN 160.

441 Tubert C, Taravini I, Flores E, Sanchez G, Prost Ma, Avale E, Tseng K, Rela L, et al. (2016),
442 Decrease of a Current Mediated by Kv1.3 Channels Causes Striatal Cholinergic Interneuron
443 Hyperexcitability in Experimental Parkinsonism. Cell Reports 16.

444 Tubert C, Taravini Irene RE, Flores-Barrera E, Sánchez Gonzalo M, Prost María A, Avale María E,
445 Tseng Kuei Y, Rela L, et al. (2016), Decrease of a Current Mediated by Kv1.3 Channels Causes
446 Striatal Cholinergic Interneuron Hyperexcitability in Experimental Parkinsonism. Cell Reports
447 16:2749-2762.

448 Varga Z, Tajti G, Panyi G (2021), The Kv1.3 K+ channel in the immune system and its "precision
449 pharmacology" using peptide toxins. Biologia Futura 72:75-83.

450 Xiong B, Zhang W, Zhang L, Huang X, Zhou W, Zou Q, Manyande A, Wang J, et al. (2020),
451 Hippocampal glutamatergic synapses impairment mediated novel-object recognition dysfunction in
452 rats with neuropathic pain. PAIN 161.

453 Xiong B, Zhang W, Zhang L, Huang X, Zhou W, Zou Q, Manyande A, Wang J, et al. (2020),
454 Hippocampal glutamatergic synapses impairment mediated novel-object recognition dysfunction of
455 neuropathic pain in rats. PAIN Publish Ahead of Print:1.

456 Xu J, Zhao W, Pan L, Zhang A, Chen Q, Xu K, Lu H, Chen Y (2016), Peimine, a main active
457 ingredient of Fritillaria, exhibits anti-inflammatory and pain suppression properties at the cellular
458 level. Fitoterapia 111:1-6.

459

460 **Figure legend**

461 **Figure 1.** Expression and cellular localization of Kv1.3 in the spinal cord of the SHAM and SNI group.
462 (A) Experimental designs and animal groups. (B) The mechanical paw withdraw threshold was
463 measured by Von Frey, and the MPWT was decreased at day 1 and continued until day 14 in the SNI
464 rats, (n = 8). (C) Compared with the SHAM group, the expression level of Kv1.3 was increased in the
465 spinal cord of the SNI rats at day 1 and continued up to day 14, (n = 6). (D) Double immunostaining
466 of Kv1.3 and iba-1 in the spinal cord. The immunoreactivity of iba-1 was increased with Kv1.3 in the
467 SNI rats, (person= Pearson Correlation Coefficient). All data are presented as mean ± SEM. $*P < 0.05$,
468 $***P < 0.001$, $****P < 0.0001$, compared with the SHAM group. D: day.

469

470 **Figure 2.** Effects of Kv1.3 blocker PAP-1 on the MPWT in the SNI rats. (A) Experimental designs
471 and animal groups. (B) MPWT was evaluated hours after the PAP-1 injection, (n = 4). (C) PAP-1
472 effectively reversed the decrease of the MPWT in the SNI rats, (n = 8). (D) Prophylactic administration
473 of PAP-1 had no effect on SNI-induced decrease of the MPWT, (n = 8). (E) PAP-1 dramatically
474 downregulated the protein level of Kv1.3 in the spinal cord, (n = 6). All data are presented as mean ±
475 SEM. $*P < 0.05$, $***P < 0.001$, $****P < 0.0001$, compared with the SNI group, $^{\#\#\#\#}P < 0.0001$,
476 compared with the SNI+saline group. D: day. Red arrow: time point of administration.

477

Figure 3. Activation of microglia in the spinal cord of the SNI rats. (A) The protein level of iba-1 was increased in the spinal cord of the SNI rats and continued until day 14, (n = 6). (B) Immunostaining of iba-1 was enhanced on day 3 and continued to day 14 in the spinal cord of the SNI rats. (C) Quantification of the mean fluorescent intensity of iba-1 positive cells in the spinal cord. (D) Quantification of the number of iba-1 positive cells per square millimeter in the spinal cord, (n = 4). All data are presented as mean ± SEM. $^{**}P < 0.01$, $^{****}P < 0.0001$, compared with the SHAM group. D: day.

Figure 4. Microglia were activated and mainly expressed as the M1 phenotype in the spinal cord of the SNI rats. (A-B) The protein levels of CD68 and iNos which are the markers of M1 phenotype microglia were increased on day 1 and continued until day 14 in the spinal dorsal of the SNI rats. (C-D) The expression levels of CD206 and Arg-1 were increased on day 1 and decreased to baseline on day 14 in the spinal cord of the SNI rats, (n=6). (E) Double immunofluorescence staining of iba-1(red) and CD68 or iNos (green) for M1 phenotype, CD206 or Arg-1 (green) for M2 phenotype. (F) Quantification of the ratio of CD68 in the iba-1 positive cells of the spinal cord. (G) Quantification of the ratio of iNos in the iba-1 positive cells of the spinal cord. (H) Quantification of the ratio of CD206 in the iba-1 positive cells of the spinal cord. (I) Quantification of the ratio of Arg-1 in the iba-1 positive cells of the spinal cord, (n=4). All data are presented as mean ± SEM. $^{*}P < 0.05$, $^{**}P < 0.01$, $^{***}P < 0.001$, $^{****}P < 0.0001$, compared with the SHAM group. D: day.

Figure 5. The NLRP3 inflammasome in the spinal cord was activated after SNI. (A-C) The expression levels of NLRP3, caspase-1, and IL-1β proteins were increased remarkably in the spinal cord of the SNI rats, (n=6). (D) Double immunofluorescence staining of iba-1 (red) and NLRP3 (green) in the

spinal cord. (E) Quantification of the mean fluorescent intensity of the iba-1 positive cells in the spinal cord, (n=4). All data are presented as mean ± SEM. *$P < 0.05$, **$P < 0.01$, ****$P < 0.0001$, compared with SHAM group.

Figure 6. Effects of PAP-1 on microglial polarization in the spinal cord. (A) The expression levels of iba-1 in the spinal cord were observably reduced after administration of PAP-1 in the SNI rats, (n = 6). (B-C) The expression levels of CD68 and iNos in the spinal cord were observably reduced after administration of PAP-1 in the SNI rats, (n = 6). (D-E) The protein levels of CD206 and Arg-1 were increased after using PAP-1 in the SNI rats, (n=6). (F) Double immunofluorescence staining of iba-1 (red) and CD68 or iNos (green) for M1 phenotype, CD206 or Arg-1 (green) for M2 phenotype.(G) Quantification of the iba-1 positive cells in the spinal cord.(H) Quantification of the ratio of CD68 in the iba-1 positive cells in the spinal cord. (I) Quantification of the ratio of iNos in the iba-1 positive cells in the spinal cord. (J) Quantification of the ratio of CD206 in the iba-1 positive cells in the spinal cord. (K) Quantification of the ratio of Arg-1 in the iba-1 positive cells in the spinal cord, (n=4). All data are presented as mean ± SEM. *$P < 0.05$, **$P < 0.01$, ***$P < 0.001$, ****$P < 0.0001$, compared with the SNI group.

Figure 7. The effects of PAP-1 on the NLRP3 inflammasome in the spinal cord of the SNI rats. (A-C) The protein levels of NLRP3, caspase-1, and IL-1β were clearly decreased in the spinal cord of the SNI rats. (n=6). (D) Double immunofluorescence staining of iba-1 (red) and NLRP3 (green) in the spinal cord. (E) Quantification of the mean fluorescent intensity of iba-1 positive cells in the spinal cord, (n=4). All data are presented as mean ± SEM. *$P < 0.05$, **$P < 0.01$, ***$P < 0.001$, compared with the SNI group.

524

525 **Figure 8.** Schematic diagram. During the development of SNI, Kv1.3 was upregulated and induced
526 microglial M1 polarization, which secreted inflammatory cytokines. Meanwhile, increased K^+ efflux
527 led to the activation of the NLRP3 inflammasome which presented as the subsequent upregulation of
528 NLRP3, caspase-1, and IL-1β.

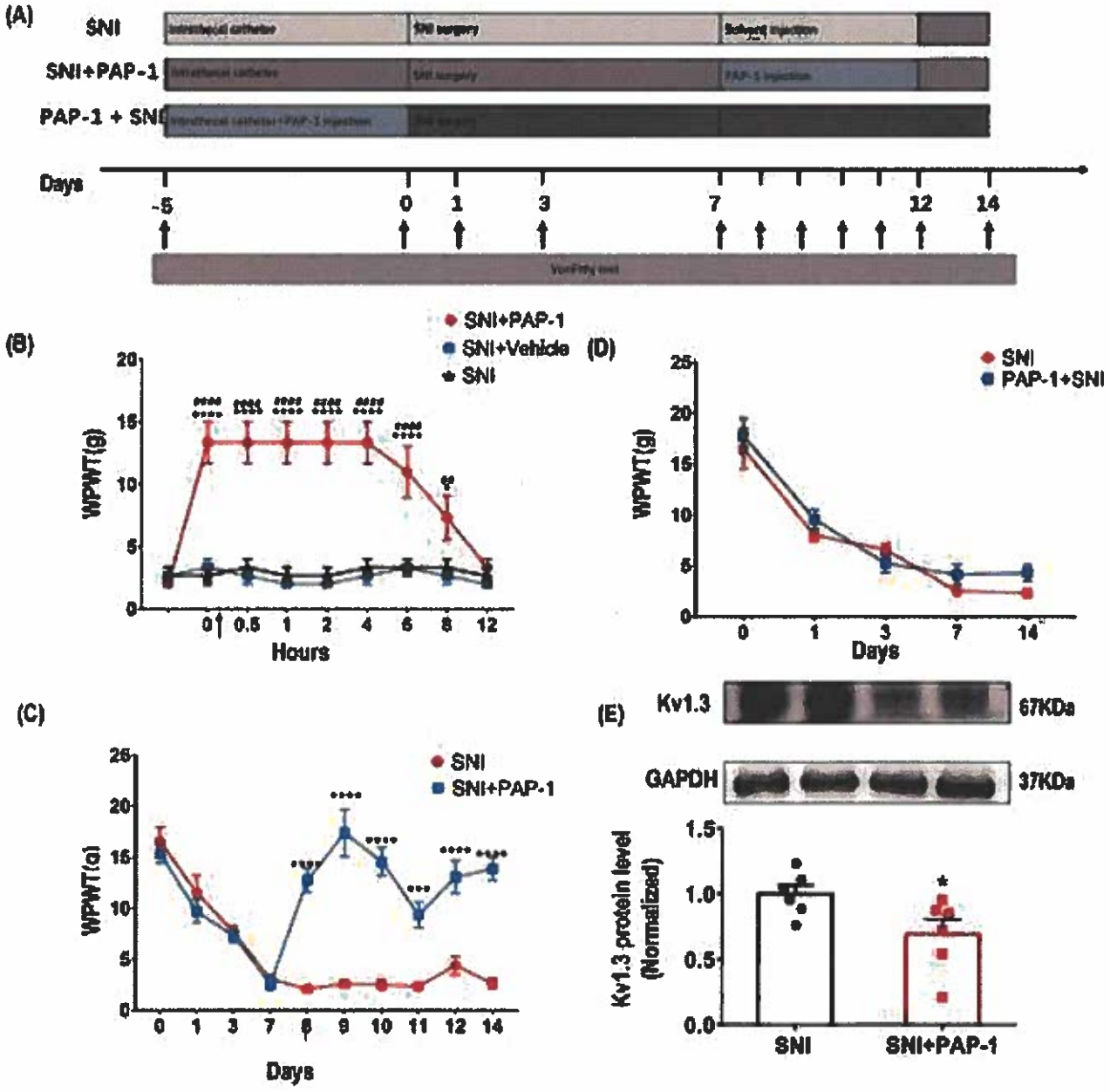

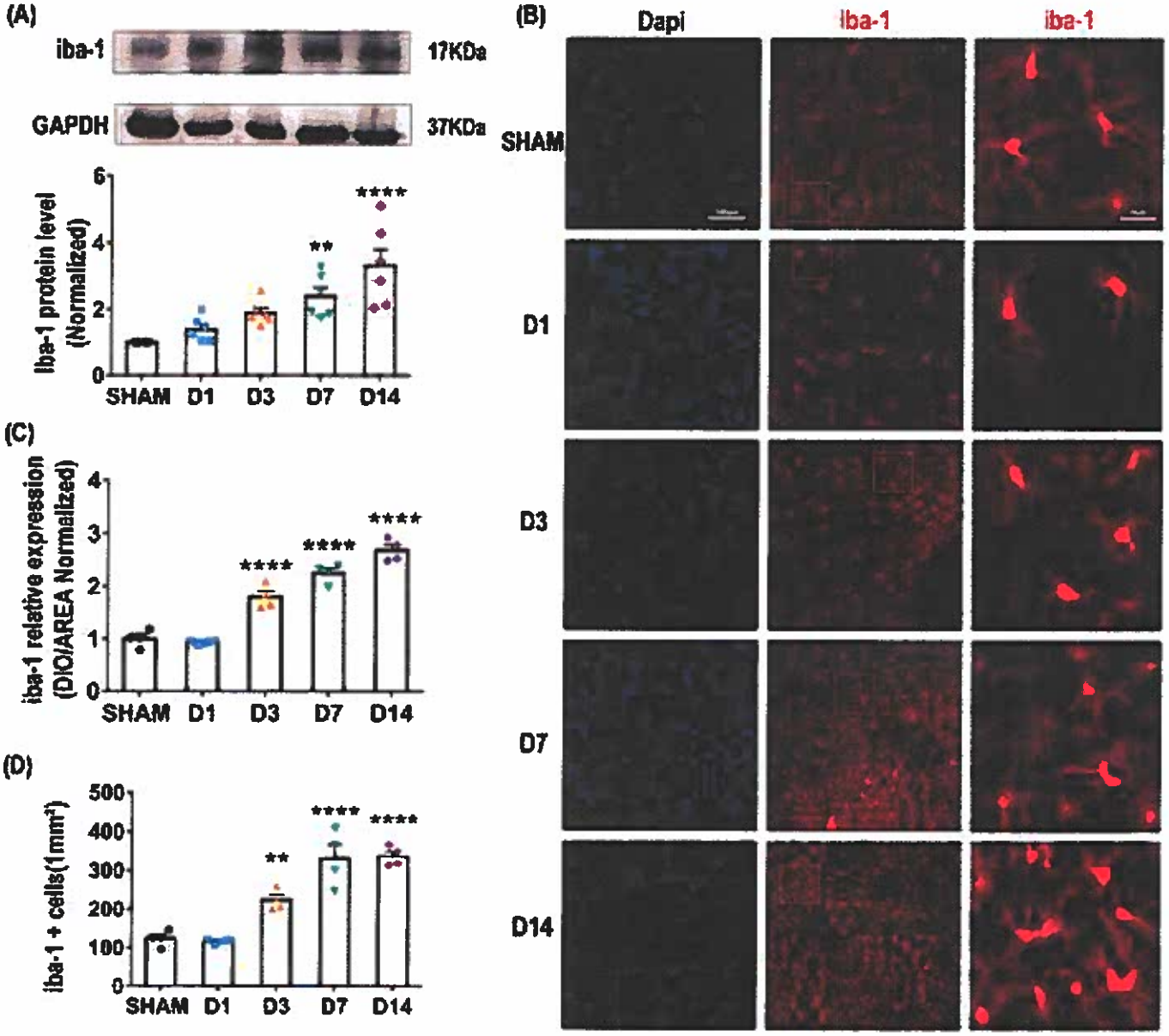

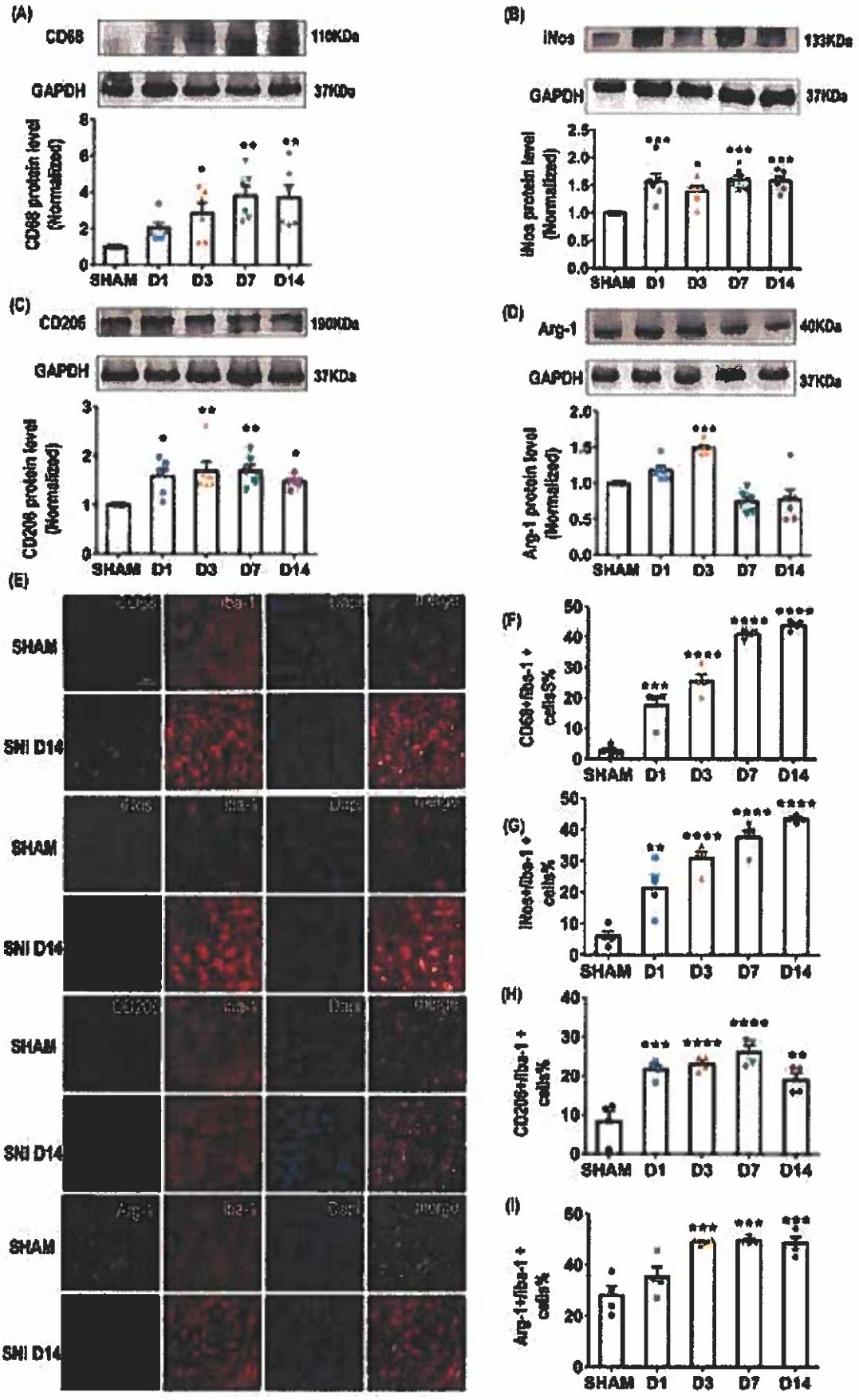

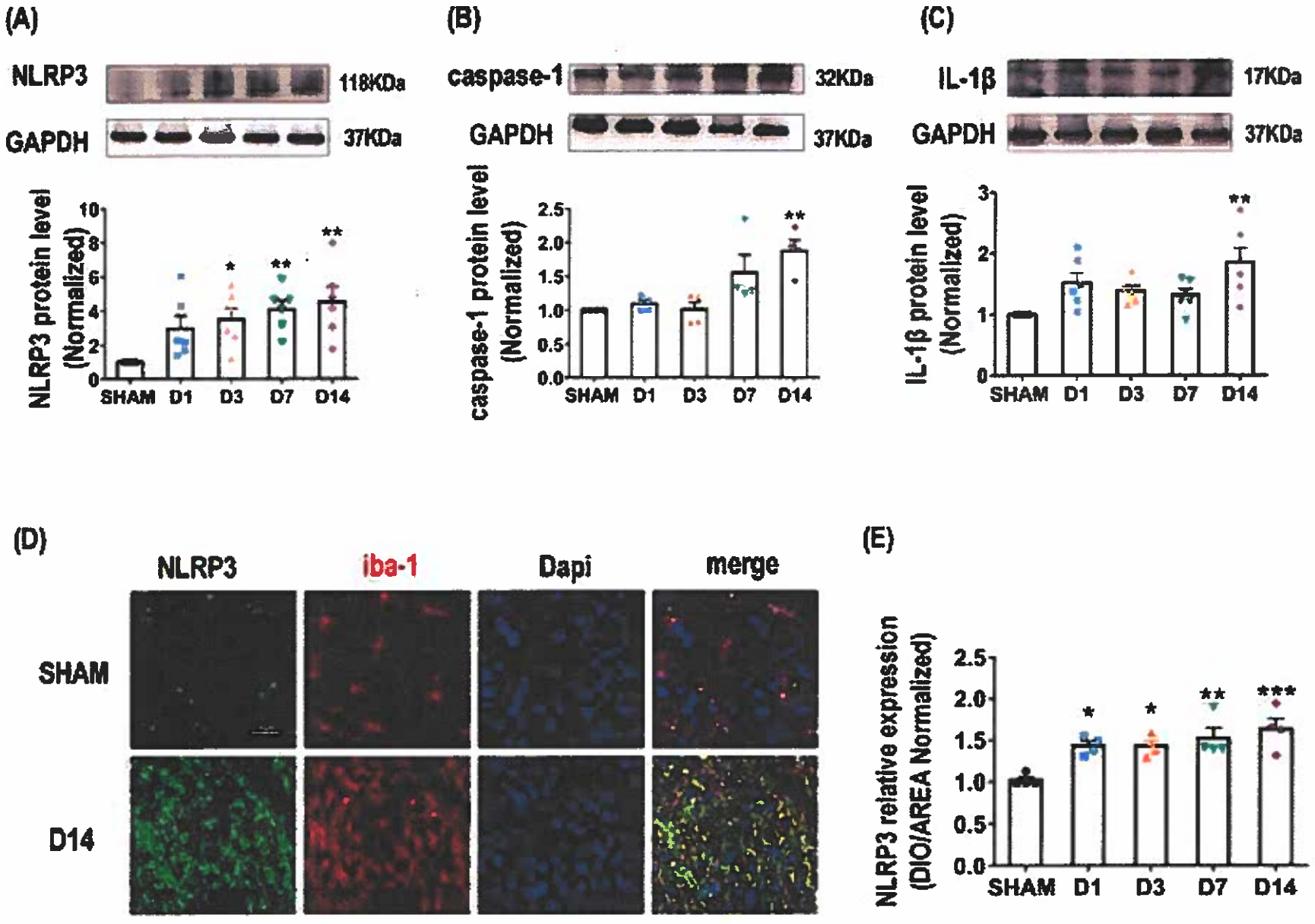

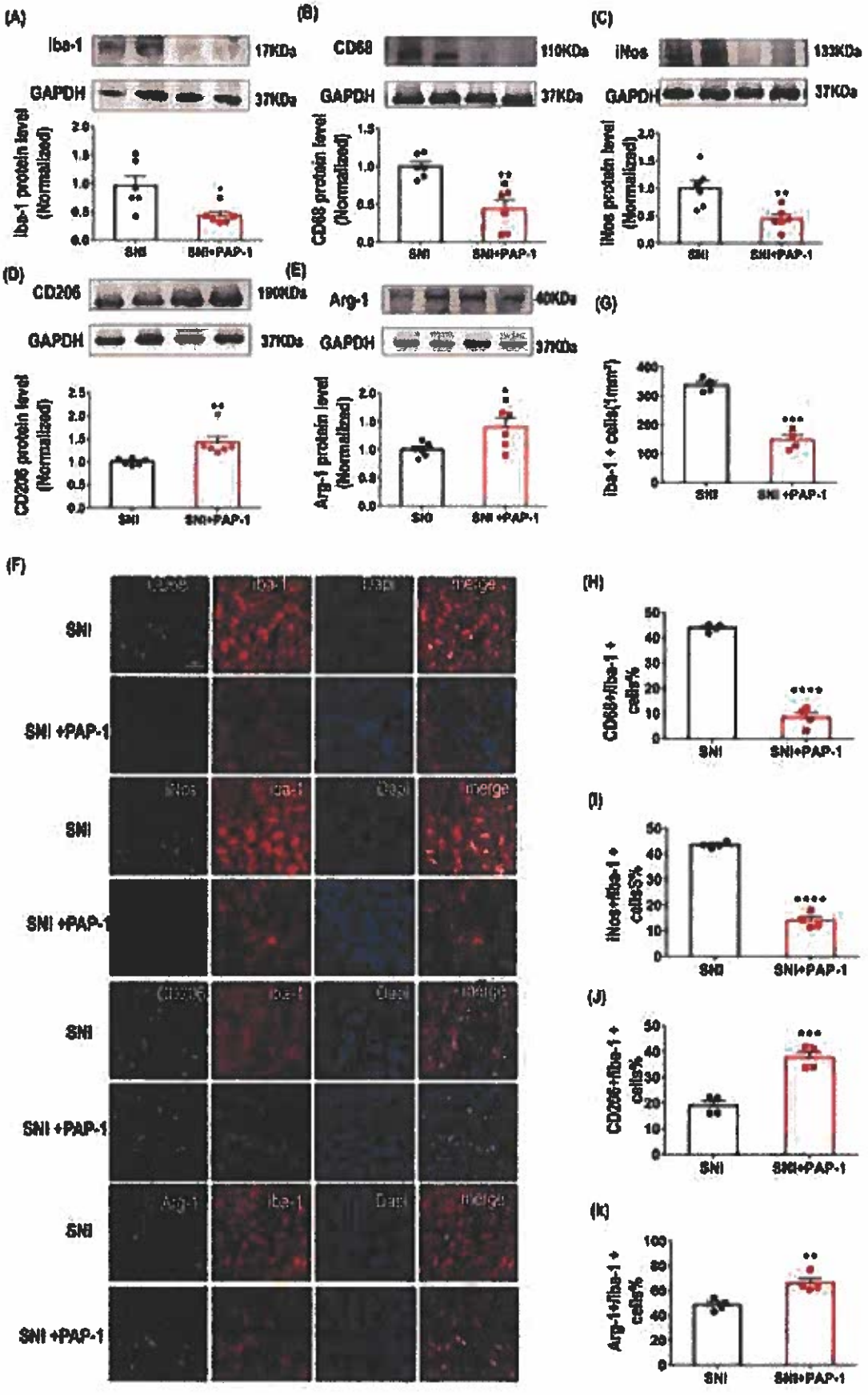

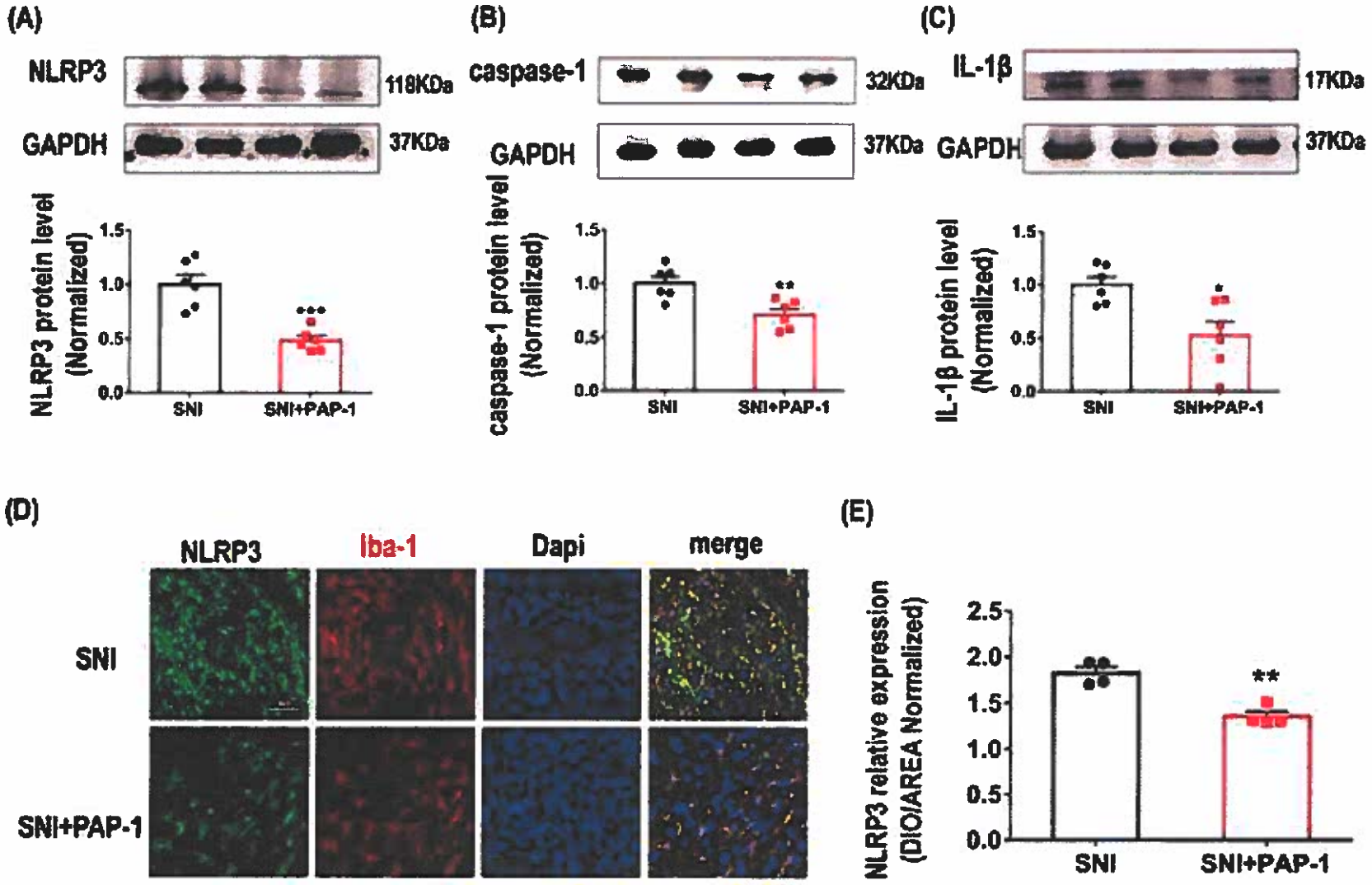

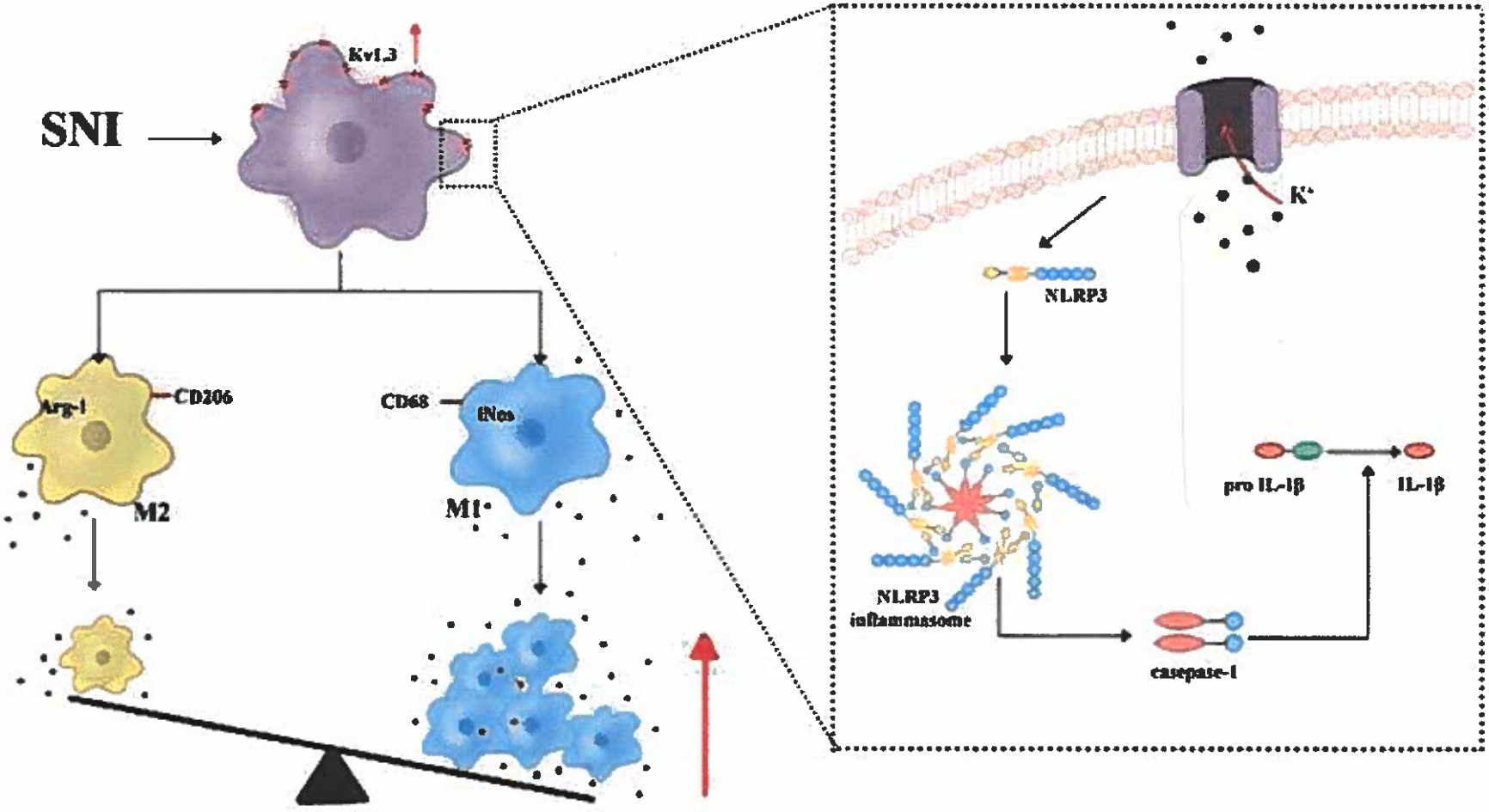

Figure

Click here to access/download;Figure;fig1.tif

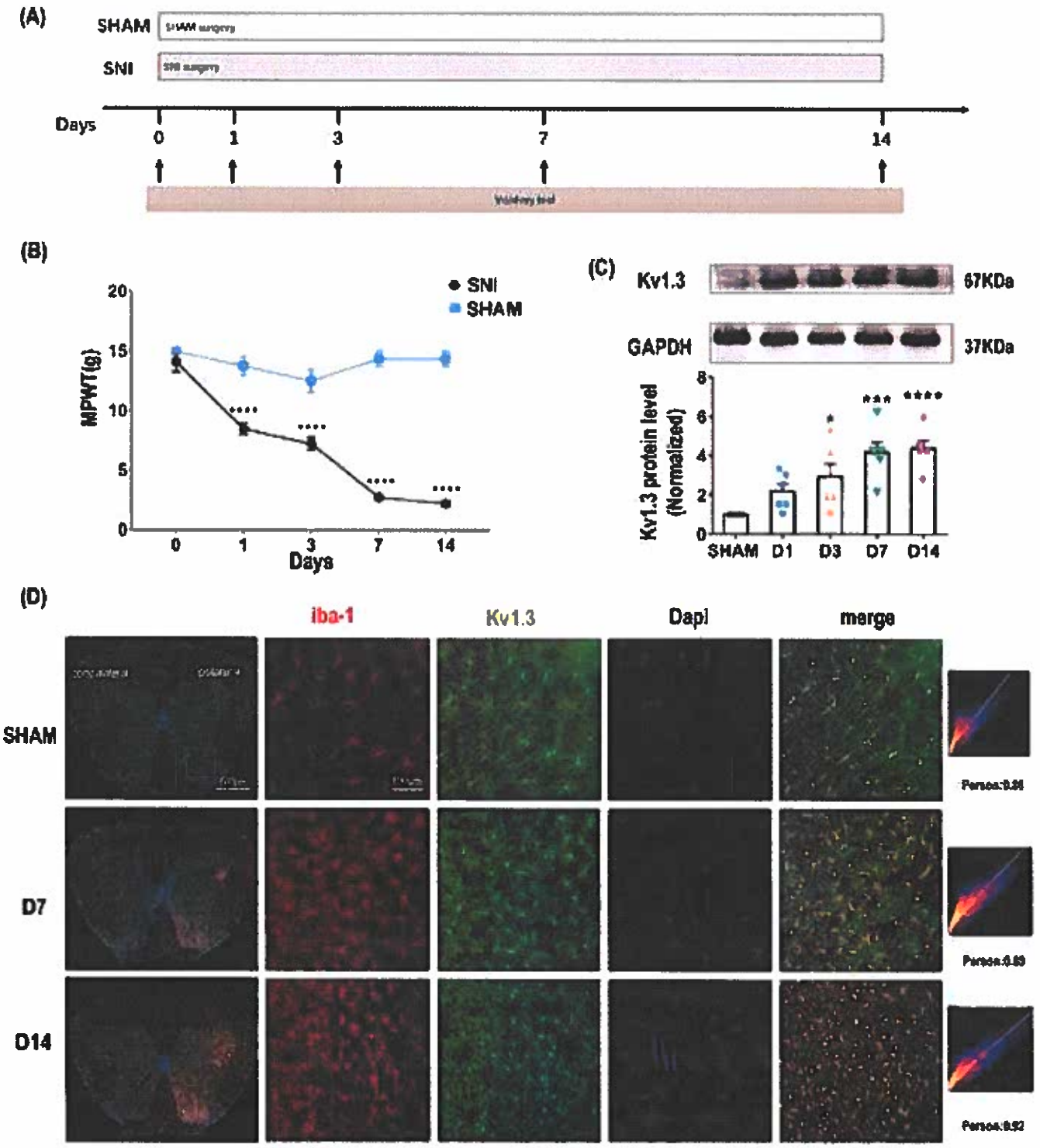

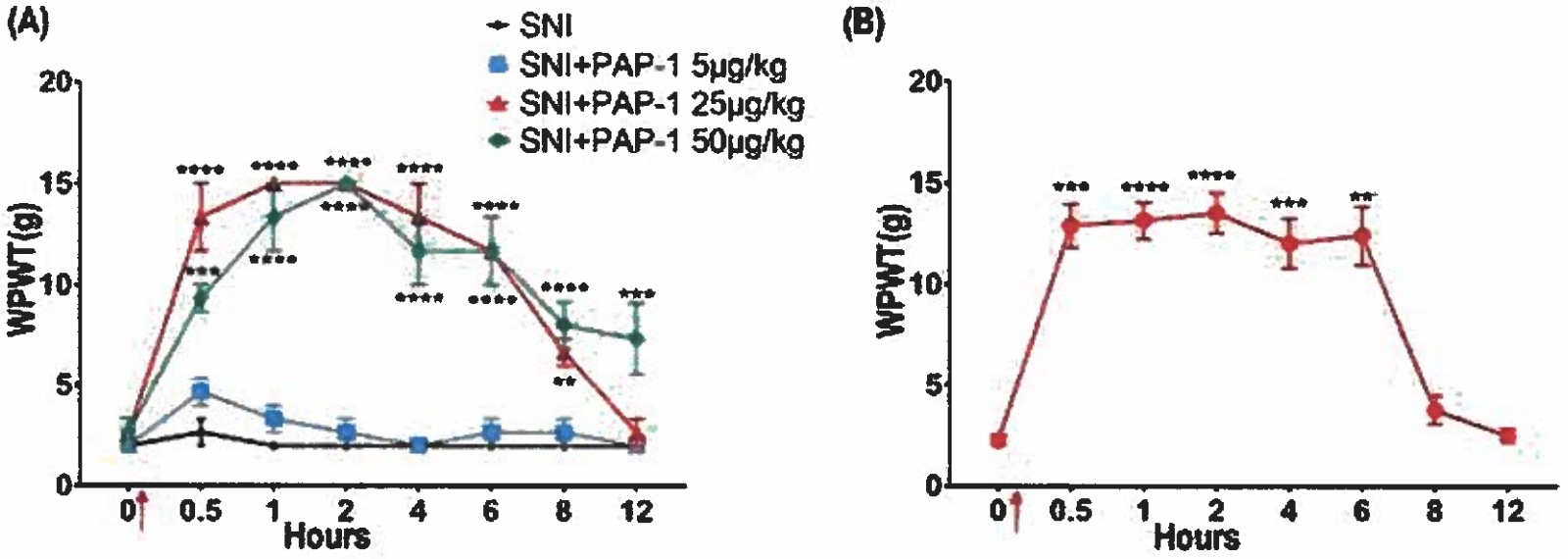

Supplementary material (former "Supporting information")

Click here to access/download;Supplementary material (former "Supporting information");figS2.tif

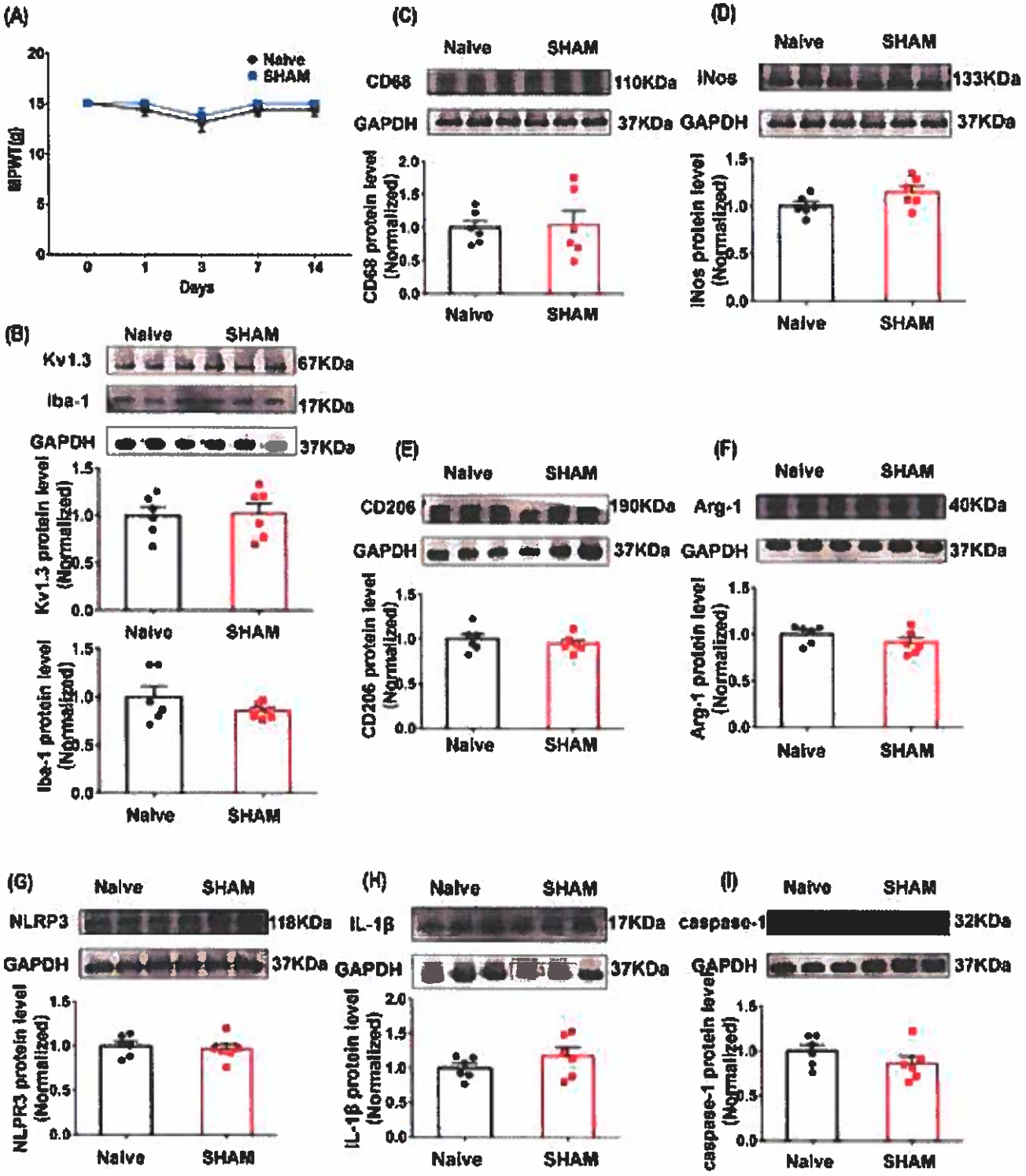

Figure 1. Effects of Kv1.3 blocker PAP-1 on MPWT in the SNI rats. (A) Effects of different doses of PAP-1 on SNI-induced decrease of MPWT, (n = 3). All data are presented as mean ± SEM. $^{**}P < 0.01$, $^{***}P < 0.001$, $^{****}P < 0.0001$, compared with the SNI group, $^{\#\#\#}P < 0.001$, $^{\#\#\#\#}P < 0.0001$, compared with the SNI group. (B) MPWT was evaluated at hours after PAP-1 injection (n = 8). The peak reached immediately after administration and lasted for 6 hours. All data are presented as mean ± SEM. $^{**}P < 0.01$, $^{***}P < 0.001$, $^{****}P < 0.0001$, compare with baseline. Red arrow: time point of administration.

Figure 2. MPWT and relevant protein expressions in the spinal cord of the Naive and Sham rats. (A) The mechanical paw withdraw threshold was measured by Von Frey, and the MPWT was decreased at day 1 and continued until day 14 in the Naive and Sham rats, (n = 8). (B) The protein levels of Kv1.3 and Iba-1 had no statistical difference between the sham and naive groups, (n=6). (C-D)There was no difference of the expression levels of CD68 and iNos had no between the sham and naive groups, (n=6).(E-F)The expression levels of CD206 and Arg-1 had no statistical difference between the sham and naive groups, (n=6). (G-I) There was no significant difference of the protein levels of NLRP3, caspase-1, and IL-1βbetween the sham and Naive group, (n=6).

Fig1 Kv1.3(sham D1 D3 D7 D14)

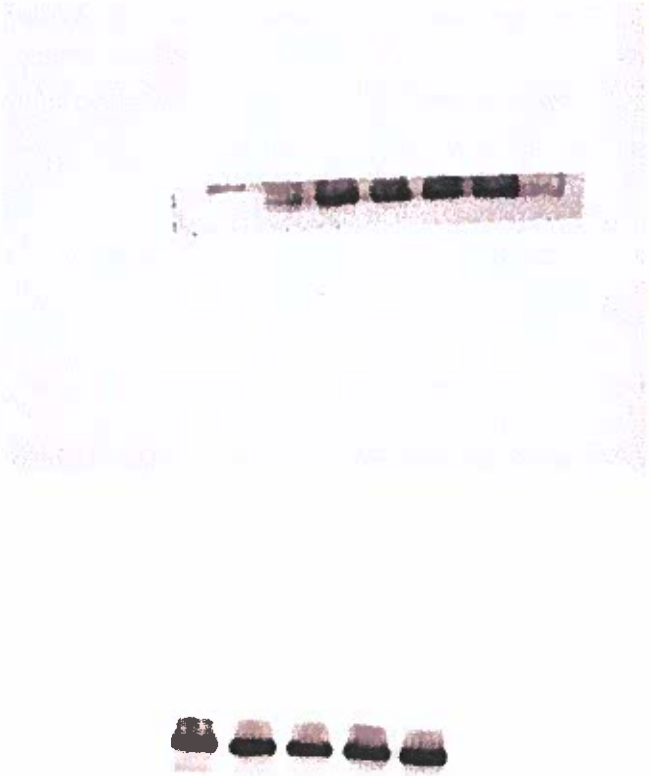

Fig2 Kv1.3 (sham d1 d3 d7 d14 d14 PAP-1 PAP-1)

Fig3 iba-1(sham D1 D3 D7 D14)

17KD

Fig4
CD68(sham D1 D3 D7 D14 D14 PAP-1 PAP-1)

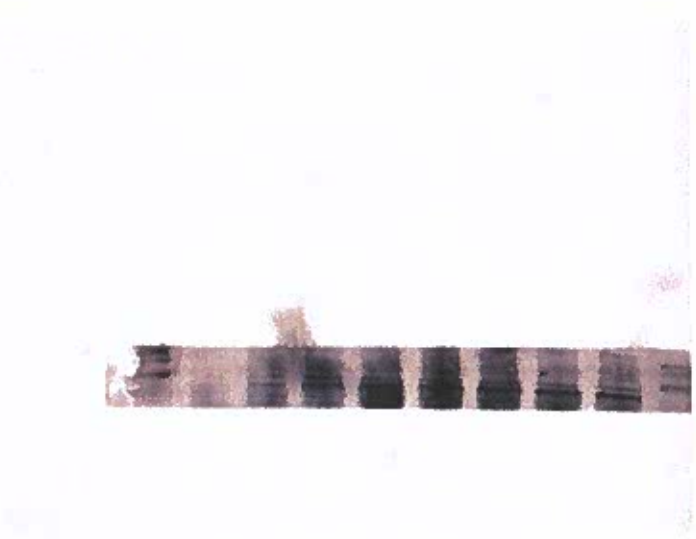

Nos(sham D1 D3 D7 D14 D14 PAP-1 PAP-1)

CD206(sham D1 D3 D7 D14)

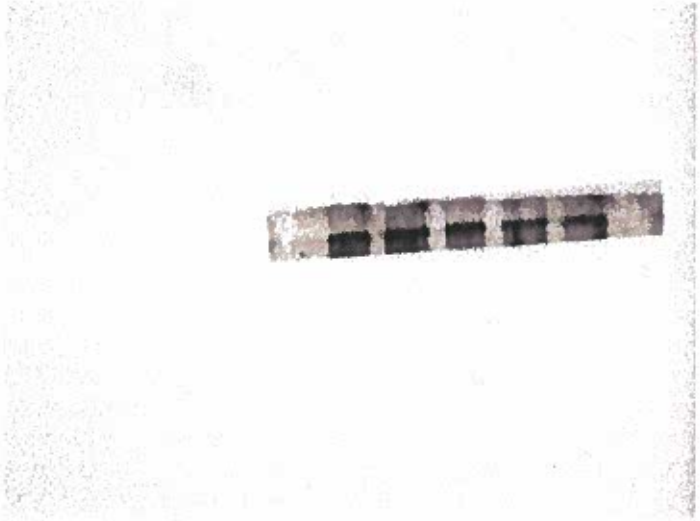

Arg-1(sham D1 D3 D7 D14)

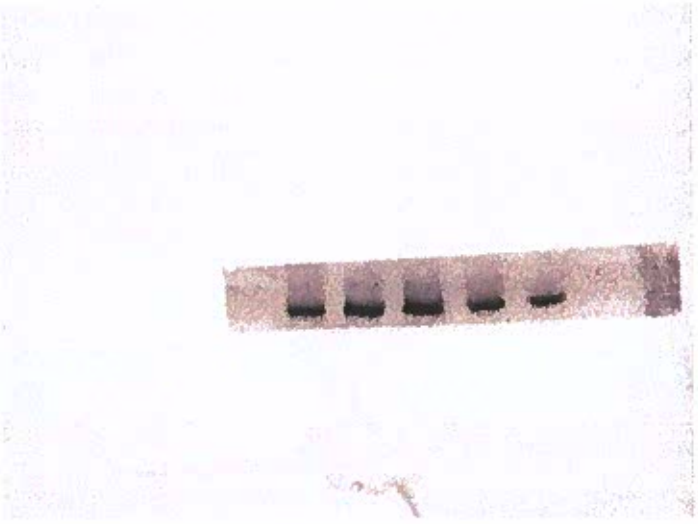

Fig5

NLRP3(sham D1 D3 D7 D14 D14 PAP-1 PAP-1)

Capase-1(sham D1 D3 D7 D14)

Il-1beta(sham D1 D3 D7 D14 D14)

Fig6

Iba-1((D14 D14 D14 PAP-1 PAP-1 PAP-1))

CD68(D14 D14 PAP-1 PAP-1 D14 D14 PAP-1 PAP-1)

Inos(D14 D14 PAP-1 PAP-1 D14 D14 PAP-1 PAP-1)

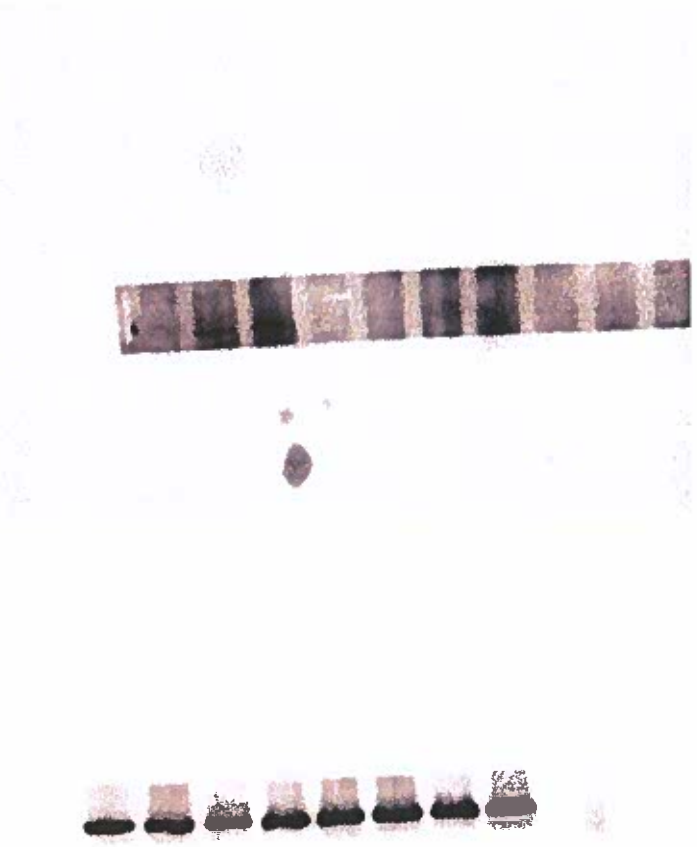

CD206(D14 D14 PAP-1 PAP-1)

Fig7

Nlrp3(D14 D14 PAP-1 PAP-1)

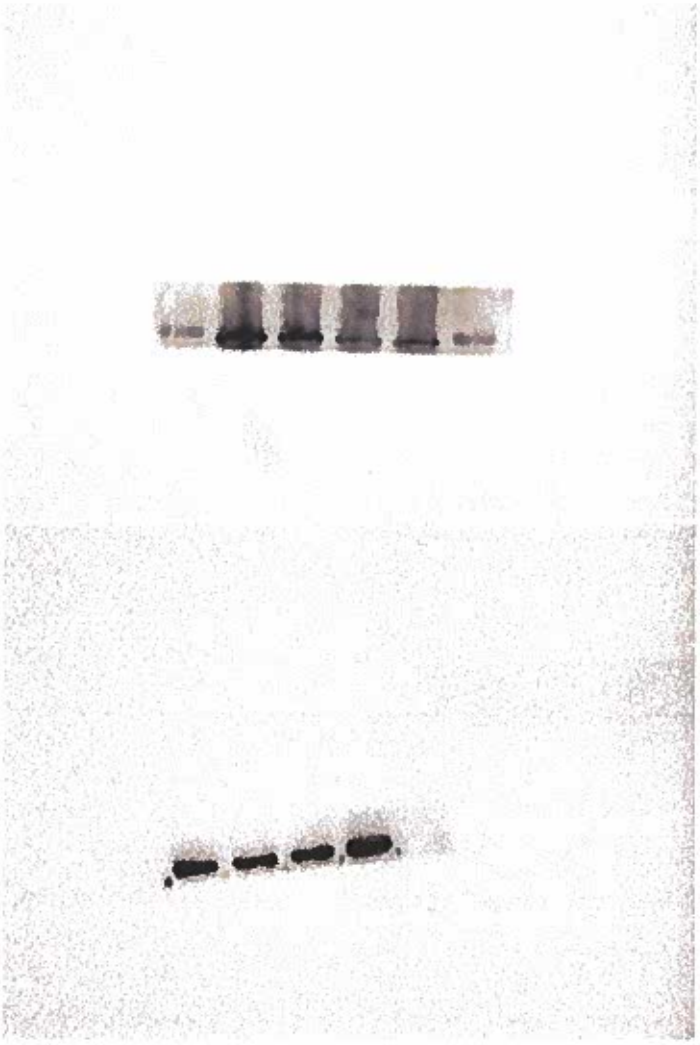

Caspase-1(D14 D14 PAP-1 PAP-1)

Il-1b(d14 d14 pap-1 pap-1 d14 d14 pap-1 pap-1)